JOURNAL OF MATERIAL SCIENCES, 31 (1996) 71–79

Low-temperature synthesized aluminosilicate glasses

Part I *Low-temperature reaction stoichiometry and structure of a model compound*

H. RAHIER, B. VAN MELE*
Department of Physical Chemistry and Polymer Science, Vrije Universiteit Brussel, Pleinlaan 2, 1050 Brussel, Belgium

M. BIESEMANS,
High Resolution NMR Centre, Vrije Universiteit Brussel, Pleinlaan 2, 1050 Brussel, Belgium

J. WASTIELS, X. WU
Department of Civil Engineering, Vrije Universiteit Brussel, Pleinlaan 2, 1050 Brussel, Belgium

The reaction below 100 °C of a dehydroxylated clay (metakaolinite: $(Al_2O_3)(SiO_2)_2(H_2O)_{0.05}$) suspended in an alkaline sodium silicate solution ($(Na_2O)(SiO_2)_{1.4}(H_2O)_x$) leads to an amorphous glassy aluminosilicate, called in this work "low-temperature inorganic polymer glass" (LTIPG or IPG).

The IPG material is amorphous according to X-ray diffraction (XRD). Its molecular structure is determined by solid state Al and Si magic angle spinning nuclear magnetic resonance (^{27}Al and ^{29}Si MAS NMR) spectroscopy. The polymer consists of SiO_4 and AlO_4 tetrahedra randomly distributed, with the restriction that no Al–O–Al bonds occur. The Al/Na ratio equals one, the overall cross-link density is almost four, and only few Si–OH groups are present.

The reaction stoichiometry is deduced from differential scanning calorimetry (DSC) and ^{27}Al and ^{29}Si MAS NMR. The inorganic polymer glass is formed by the low-temperature reaction of silicate and metakaolinite in a one to one ratio, according to the following overall reaction equation

$$(Na_2O)(SiO_2)_{1.4}(H_2O)_x + (Al_2O_3)(SiO_2)_2(H_2O)_{0.05} \xrightarrow{\text{aq.}(<100\,^\circ C)} (Na_2O)(Al_2O_3)(SiO_2)_{3.4}(H_2O)_z$$

with z about 0.4.

Mechanical testing shows that the ultimate compressive strength of the inorganic polymer glass corresponds with the stoichiometric silicate/metakaolinite one to one mixing ratio.

1. Introduction

In recent years, the interest in inorganic polymers in general is growing. Inorganic polymers may consist of linear molecules but also of extremely cross-linked networks. In general, highly cross-linked materials are rather brittle and often processed at elevated temperatures in the (partially) molten state where they possess a high viscosity complicating their use as a matrix for composites. Consequently much effort has been done to lower the fabrication temperature, e.g. via the sol–gel method [1, 2].

The amorphous aluminosilicate in this work is synthesized below 100 °C, and will be denoted as "low-temperature inorganic polymer glass" (LTIPG or IPG). The material's structure and its nomenclature will be justified later on.

The two constituents of the reaction mixture are a dehydroxylated clay and an alkaline silicate solution. The reaction is exothermic and transforms the reaction mixture from a suspension into solid IPG and a residue, which is mainly water. The rheology of this castable suspension can be tuned by altering the

* Author to whom correspondence should be addressed.

0022–2461

properties of the two reactants or their mixing ratio (composition). As a result, a lot of processing techniques are suitable for the production of IPG (casting, pressing, impregnation of fibres, pultrusion). Because of a hardening reaction below 100 °C and a flexible processability, even organic additives like polypropylene fibres can be worked in. So, the process ability and the hardening process of this material can be compared to the cure of organic resins. However, the mechanical properties and chemical (degradation) stability are better, especially at elevated temperatures. Besides, an important difference of this way of preparation, compared to the sol–gel technique, is that a material with good mechanical properties is obtained without the need for additional drying and sintering. For the foregoing arguments, LTIPG is a promising new material [3, 4].

For optimization of the processing parameters and the properties of IPG, a thorough understanding of the chemical reaction and the relationship between microstructure and macroscopic properties of IPG is needed. Experimental variables of importance to establish these "structure–property" relations are summarized in Scheme 1.

Scheme 1: Parameters of importance for the "structure –property" relations of LTIPG

1. Reactants:	A. Clay	a. Nature of the clay
		b. Dehydroxylation process
	B. Silicate solution	a. Nature of the cation
		b. Cation/Si ratio
		c. Water content
		d. Silicate preparation
2. Chemical reaction	A. Mixing ratio and reaction stoichiometry	
	B. Reaction kinetics	
	C. Reaction mechanism [5]	
	D. Chemorheology	
3. Structure of IPG:	A. Short range order (molecular structure on nearest neighbour level) [6]	
	B. Intermediate range order (molecular structure over several nearest neighbour distances) [6]	
	C. Long range order (arrangements of atoms over distances of 1 nm or more – crystallinity) [6]	
	D. Global range order (porosity, homogeneity, inclusion of particles, morphological aspects) [6]	
	E. Thermal history and processing conditions	

In a first paper, a few important parameters of Scheme 1 will be investigated on a well defined model system. The stoichiometry of the reaction between one specific sodium silicate and a representative calcined clay (metakaolinite) will be investigated with differential scanning calorimetry (DSC). The bound water content of metakaolinite and LTIPG will be measured with thermogravimetric analysis (TGA). The molecular structure of LTIPG will be determined by solid state ^{27}Al and ^{29}Si nuclear magnetic resonance (NMR), to complete also the reaction equation and stoichiometry from a molecular viewpoint. Mechanical testing will enable the investigation of some "structure–property" relations.

2. Experimental procedure

2.1 Raw materials and processing

The kaolinite used is a well crystallized kaolin (KGa-1) [7] with a theoretical bound water content of 13.95 wt %. To obtain metakaolinite this kaolinite is heated at 700 °C for one hour. The residual bound water is 0.38 wt %. This metakaolinite (denoted as Mk) is used in all investigations except for the mechanical testing, where a metakaolinite (coded A91) produced with a pilot scale rotary kiln from AGS is used with a metakaolinite content of about 85%. The remaining 15 wt % consists of non-reactive minerals.

The different sodium silicate solutions (denoted as Sil with composition (in molar ratio): $SiO_2/Na_2O = s = 1.4$; $H_2O/Na_2O = w$, variable) are prepared by dissolving amorphous silica in the appropriate alkaline solution. This mixture is heated at 80 °C till a clear solution is obtained.

The LTIPG samples for MAS NMR and XRD (powdered before analysis) are obtained by mixing the appropriate amount of silicate solution ($H_2O/Na_2O = 10$) and Mk, and curing this mixture in a closed mould at room temperature for at least two days. The DSC samples ($H_2O/Na_2O = 10$) are freshly mixed.

The specimens for the mechanical testing contain quartz sand (Mol, Belgium) as a filler material. The grade has a mean particle size of 240 μm (coded M32). All raw materials are mixed in a planetary mixer Hobart N50G, and are cast into a mould of 20 × 160 × 280 mm. The closed mould is heated at 60 °C for 24 h. After cooling down to ambient temperature the hardened plate is cut with a diamond saw into samples for mechanical testing (approximate size: 20 × 30 × 40 mm). Until the moment of testing three days later, three samples of each composition are conditioned in a dry atmosphere at 40 °C and three samples are immersed in water at 25 °C. The different compositions for mechanical testing are given in Table I. The samples for the DSC measurements in Section 3.3 have the same composition, but sand is excluded.

Note that in the text molar ratios will always be used. One mole of silicate solution contains one mole

TABLE I Composition of specimens for mechanical testing

Sil/Mk	Na/Al	H_2O/Na_2O[a]	M32/A91[b]
0.8	0.8	13.9	2.4
1.0	1.0	11.9	2.6
1.2	1.2	10.7	2.7
1.4	1.4	10.0	2.8
1.7	1.7	8.9	3.1

[a] The H_2O/Na_2O molar ratio w for the different silicate solutions is varied, while their SiO_2/Na_2O molar ratio s is always 1.4.
[b] The filler (M32) to clay (A91) weight ratio.

of Na_2O and is defined as $(Na_2O)(SiO_2)_{1.4}(H_2O)_x$. It should be pointed out that x contains only the bound water in the solution and is different from w. One mole of kaolinite and Mk are defined as $(Al_2O_3)(SiO_2)_2(H_2O)_2$ and $(Al_2O_3)(SiO_2)_2(H_2O)_{0.05}$ respectively.

2.2 Analytical techniques

2.2.1 Differential scanning calorimetry

The measurements are performed on a Perkin Elmer DSC 7. Reusable high pressure stainless steel sample pans are taken. Gold coated sample pans (same type) are used too, to check that no reaction between the alkaline sample and the sample pan takes place. No differences are observed between the reaction exotherm in golden or stainless steel sample pans. The scans are performed between -60 and 300 °C with a scan rate of 5 °C min^{-1}. For the isothermal experiments the sample is scanned from 20 °C at 20 °C min^{-1} to the isothermal temperature.

For the calculation of the reaction enthalpy a straight baseline is used. Each reported reaction enthalpy is the mean value of three independent measurements. The maximum difference for the reaction enthalpy per gram of reaction mixture is 7%.

2.2.2 Thermogravimetric analysis

The thermobalance used is a Perkin Elmer TGA 7. The purge gas is He. The weight loss to determine the total or residual bound water content of kaolinite or metakaolinite respectively, is measured with the following temperature programme: the sample is dried at 250 °C for 3 h, then the temperature is raised (at 50 °C min^{-1}) to 1000 °C for 4 h. Only the weight loss after the drying step is taken into account. This procedure results in a total bound water content for kaolinite of 13.76% (in excellent agreement with the theoretical total water content of 13.95%) and a residual bound water content for metakaolinite of 0.38%. The same procedure is followed to determine the bound water content of LTIPG.

2.2.3 X-Ray diffraction

XRD diffractograms of powdered samples of kaolinite, Mk and LTIPG are registered on a Siemens 500 Kristalloflex, generating a Ni-filtered CuK_α radiation with an applied voltage of 40 kV and a current of 30 mA.

2.2.4 Nuclear magnetic resonance spectroscopy

Spectra for ^{29}Si and ^{27}Al are obtained on a Bruker AC250 spectrometer operating at 49.70 and 65.18 MHz for the ^{29}Si and ^{27}Al resonance frequencies, respectively. The spectrometer is interfaced with an Aspect-3000 computer and equipped with a MAS broad-band probe for the solid state experiments.

Chemical shifts are referenced to external TMS in $CDCl_3$ for the ^{29}Si nuclei and to external aqueous $AlCl_3$ for the ^{27}Al nuclei. The chemical shift values are calculated by taking the midpoint of the signal at half height. The accuracy is 0.5 p.p.m.

Rotors of 7 mm diameter and a spinning rate of 5 kHz are used for the solid state experiments. Typically, ^{29}Si spectra are obtained over a spectral width of 11.1 kHz (acquisition time = 0.2 s), with 1000 scans and a relaxation delay of 2 s. The ^{27}Al spectra are acquired over a spectral width of 55.6 kHz, (acquisition time = 0.04 s), with 400 scans and a relaxation delay of 0.5 s.

2.2.5 Mechanical testing

Mechanical testing is performed on an Instron 1195 universal testing machine. Compressive tests are executed following ASTM C349-82 (compression surface 40 × 20 mm, specimen height 30 mm). For each post-curing condition (dried or immersed) and each composition, three identical specimens are tested. The immersed specimens are tested immediately after removal from the water, so that they can be considered to be saturated to equilibrium when tested.

3. Results and discussion

3.1 Stoichiometry of the low-temperature reaction – DSC study

The exothermic reaction of metakaolinite (Mk) with the sodium silicate (Sil) can be studied with differential scanning calorimetry. Typical DSC thermograms at 40, 50 and 60 °C for a Sil/Mk ratio of one are shown in Fig. 1, indicating that a fast cure is realistic in isothermal conditions at relatively low temperatures (around 60 °C). The maximum exothermic heat flow (and thus the maximum reaction rate) is observed at the beginning of the reaction and already after four hours of reaction at 60 °C the partial reaction enthalpy (ΔH_r(iso) = -190 J g^{-1}) is almost the same as the total reaction enthalpy in a non-isothermal experiment (ΔH_r(non-iso) = -230 J g^{-1}), as shown in Fig. 2(a). Here, the maximum reaction rate is still observed below 100 °C.

It should be stressed that neither metakaolinite nor the silicate solution exhibit transitions or react alone

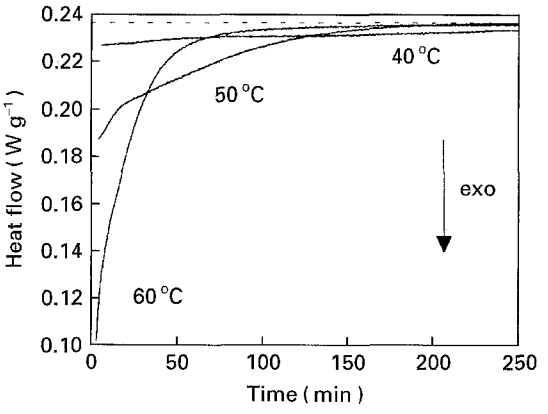

Figure 1 DSC thermograms for the isothermal cure (40, 50 and 60 °C) of the reaction mixture with Sil/Mk = 1. The dashed line represents the base line.

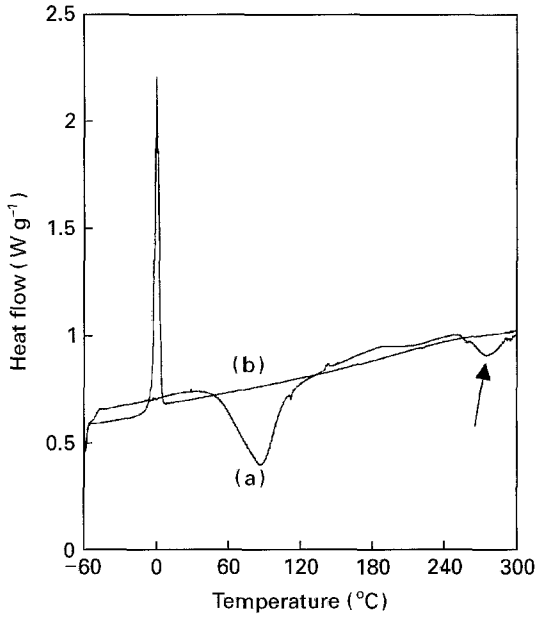

Figure 2 Non-isothermal DSC thermogram (5 °C min^{-1}) of the reaction mixture with Sil/Mk = 1: (a) first heating; (b) second heating.

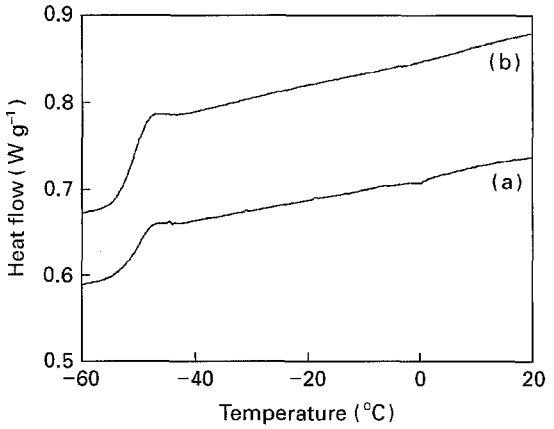

Figure 3 DSC thermogram (first heating) of the glass transition for: (a) the uncured reaction mixture with Sil/Mk = 1; (b) the silicate solution.

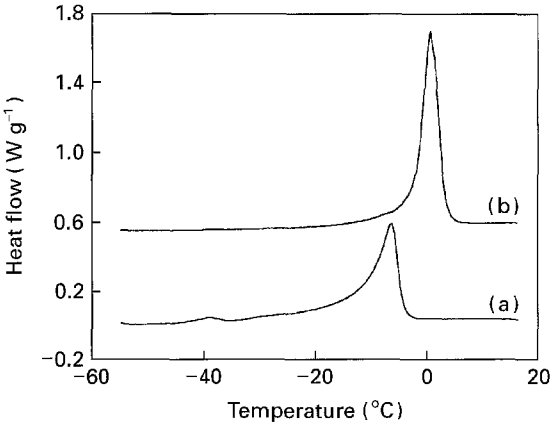

Figure 4 DSC thermogram (second heating after polymerization) of the melting of remaining water: (a) Sil/Mk = 1.3; (b) Sil/Mk = 0.7.

in the temperature range of the reaction exotherm. The reaction signal consists of two well separated exotherms, one far below and one above 200 °C (see arrow in Fig. 2(a)). This probably indicates a complicated reaction mechanism and kinetics. Only the reaction with the low-temperature exotherm will proceed to a significant extent in an isothermal cure at 60 °C for 24 h (which is the cure procedure of the specimens for mechanical testing). The reproducibility of the high-temperature part of the DSC-exotherm is poor, but seems to be influenced to a large extent by the particle size of the dehydroxylated clay. However, for the model compounds used in this work, the first part of the reaction exotherm is predominant and of importance for attaining the final mechanical properties. For these reasons no quantitative interpretation of the second DSC-signal has been done yet. A detailed study of the reaction kinetics and mechanism is in progress.

After reaction in the first DSC heating, IPG and some non-bound water remain. Fig. 2(b) shows a second heating curve (after polymerization). The endothermic peak is the melting of this non-bound water.

The glass transition T_g of the polymer glass is not observed during the second scan. It will be shown that after polymerization and evacuation of residual water, T_g is found at a much higher temperature (around 650 °C) [8]. During the first heating no melting endotherm from the silicate solution is observed. On the contrary, the initial reaction mixture has a T_g at about − 50 °C. Fig. 3(a) shows that T_g of the reaction mixture coincides with T_g of sodium silicate in Fig. 3(b). It is obvious that Mk in the mixture is not influencing the initial T_g-value of the sodium silicate, so that Mk can be considered as a filler (at the beginning, but also in non-stoichiometric conditions at the end of the reaction, see discussion later on).

In the second heating run after polymerization, a melting point depression is observed if Sil/Mk ratios bigger than one are used (see Fig. 4(a)), and not in the case of Sil/Mk ratios smaller than one (Fig. 4(b)) where melting occurs at the same position as in the one-to-one mixing ratio (Fig. 2(b)).

A more definite value for this indication of the stoichiometric Sil/Mk ratio can be deduced from the calculated reaction enthalpy of the first reaction exotherm. Fig. 5 shows this reaction enthalpy as a function of the Sil/Mk ratio k, which is equal to the Na/Al ratio. A maximum reaction enthalpy is observed for a ratio equal to one (Fig. 5(a)). This value is confirmed in Fig. 5(b) and 5(c). The reaction enthalpy per gram Mk (Fig. 5(b)) should be constant if an excess of silicate is added to the Mk, this is for ratios of k above the stoichiometric value. Furthermore, the reaction enthalpy seems to vary linearly with the Sil/Mk ratio for values less than one. The reaction enthalpy per gram silicate (Fig. 5(c)) on the other hand should be constant if an excess of Mk is added to the silicate. For very low Sil/Mk ratios, the mixing becomes experimentally difficult and the reaction could be incomplete. Homogeneous samples with a Sil/Mk ratio less than 0.54 could therefore not be investigated. So, from DSC measurements it can be concluded that the stoichiometric Sil/Mk ratio is one ($k_{st} = 1$).

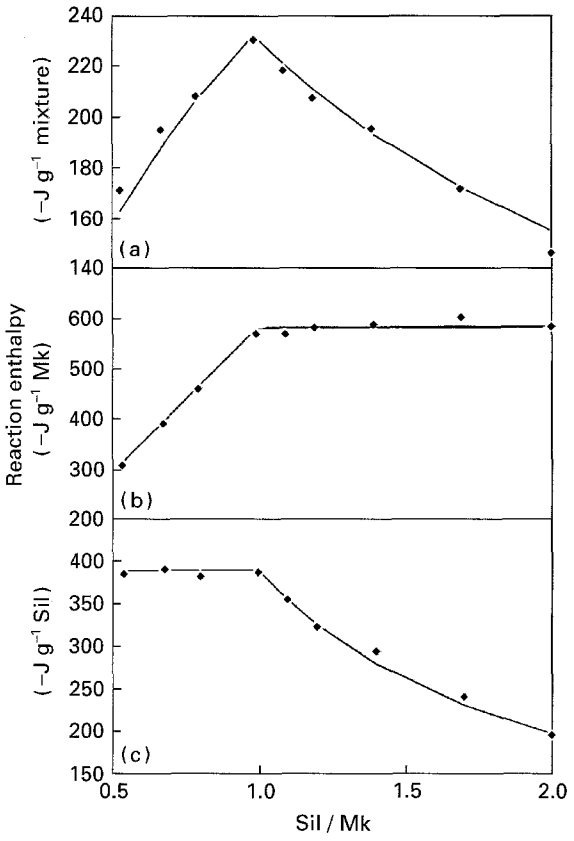

Figure 5 Reaction enthalpy ΔH_r(non-iso) as a function of the Sil/Mk ratio: (a) reaction enthalpy per gram mixture; (b) reaction enthalpy per gram Mk; (c) reaction enthalpy per gram Sil. The curves in (a) and (c) indicate the expected trend according to (b).

3.2 Structure of the low-temperature inorganic polymer glass – XRD and NMR study

The structure of IPG is important for its final (thermo) mechanical properties. Different aspects of the structure of IPG have to be taken into account (see also Scheme 1). On a macroscopic level, the porosity and homogeneity of the material should be investigated. On a smaller scale, crystallinity is very important (long range order). These two levels, but especially the first one, are largely influenced by the processing conditions and the thermal history of the material. On the molecular scale, we are interested in the co-ordination of Al and Si and in the way the building units such as SiO_4 tetrahedra are linked to each other (short and intermediate range order). The presence of water in the final structure and its chemical nature is of importance too. These molecular structural levels are strongly determined by the low-temperature chemical reaction.

This paper mostly deals with the molecular structure of IPG restricted to the chemical short range order (NMR; Scheme 1.3.A.), but first the amorphous nature of the IPG will be demonstrated. Fig. 6 shows the X-ray diffractogram of powdered kaolinite, Mk and LTIPG. XRD clearly demonstrates that the original crystallinity of kaolinite is destroyed by the thermal dehydroxylation process into Mk. The absence of sharp diffraction peaks in the spectra of Mk and LTIPG, except for a trace of the TiO_2 impurity corresponding to a distance of 0.352 nm [7], indicates that

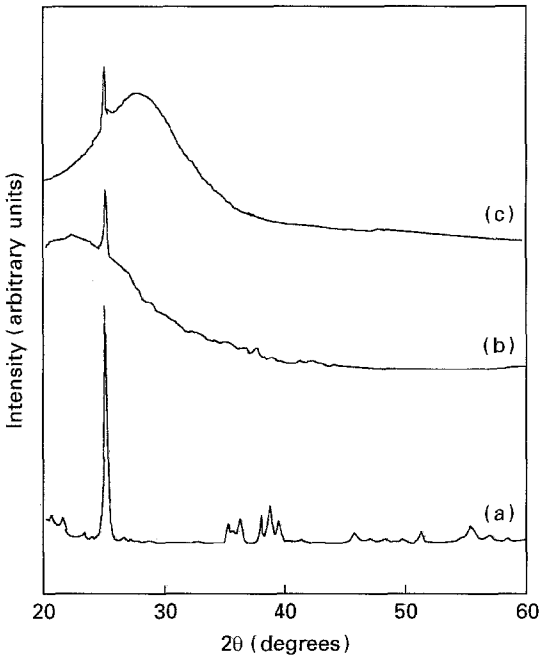

Figure 6 X-ray diffractograms of: (a) kaolinite; (b) metakaolinite (smoothed); (c) LTIPG (smoothed).

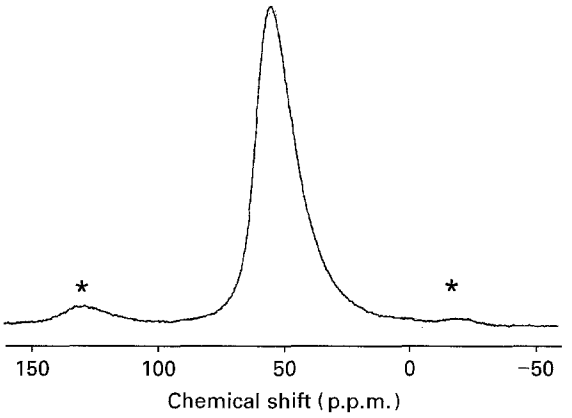

Figure 7 Typical ^{27}Al MAS NMR spectrum of LTIPG. *spinning side bands.

on the long-range scale (see Scheme 1.3.C.) no periodic repetition or ordering is introduced by the low-temperature conversion of Mk into LTIPG, so that both materials can be considered amorphous. The broad peaks detected by NMR (see discussion later on) indirectly confirm the amorphous character of LTIPG.

For all initial Sil/Mk ratios of the reaction mixture, the ^{27}Al MAS NMR spectrum of LTIPG (Fig. 7) shows one single peak centred at 58 p.p.m. with a full width at half maximum (FWHM) of 16 p.p.m. The peak lies within the chemical shift range of tetrahedral Al surrounded by four SiO_4 groups (from about 52 to 70 p.p.m. [9]). This finding is in agreement with Loewenstein's rule of "Al–O–Al avoidance" [9] and also implies that the cross-link density of Al is four (defined here as the number of bridging oxygen atoms and also called connectivity [9]). In analogy with a SiO_4 tetrahedron (see later), the short range chemical environment of Al can be written as q^4(4Si), where $q^{n'}$(m'Si) denotes an AlO_4 tetrahedron with n' bridging oxygen atoms containing m' Al–O–Si links [9]. It should be

emphasized that the chemical shift range for q^4(4Si) is not overlapping with other Al environments, so that the assignment is unambiguous. Since only a signal for tetrahedral Al is observed in LTIPG, it seems that the other Al sites present in Mk, Al^V (about 35 p.p.m.) and Al^{VI} (about 0 p.p.m.), are completely transformed into Al^{IV} by the low-temperature reaction. The same is observed in the reaction of Mk with NaOH. This is in line with the findings of Rocha and Klinowski [10] that treating Mk with KOH transforms five- and six-co-ordinated Al into four-co-ordinated Al.

According to the DSC results, the stoichiometry of the reaction suggests that for each Al present in metakaolinite one cation (Na^+) from the silicate should be added. This previous finding can be understood now in terms of the ^{27}Al NMR results. Since Al is tetrahedrally co-ordinated, Na^+ is needed in a one-to-one ratio to compensate the negative charge introduced by each AlO_4 group.

Finally, it should be pointed out that the intensity of the ^{27}Al MAS NMR signal of LTIPG spectacularly increased compared to Mk, suggesting a more symmetrical environment around the ^{27}Al quadrupolar nucleus in LTIPG. The FWHM-value of 16 p.p.m. of the ^{27}Al MAS NMR signal lies close to that of crystalline materials (e.g. kaolinite FWHM = 12 p.p.m. [11]). The ^{27}Al MAS NMR signal of amorphous materials (such as Mk) can be so broad that the signal is not or only partially detected [9]. The relatively small spinning side bands and the fact that the ^{27}Al peak is symmetric (see Fig. 7) also indicate that the short range chemical environment around the quadrupolar Al nucleus is symmetric. The short range symmetric order around Al is not in contradiction with the amorphous nature of LTIPG on the XRD scale, and should not be confused with the existence of any crystalline long range order.

A typical ^{29}Si MAS NMR spectrum of LTIPG shows a peak centred at -91 p.p.m. with a FWHM of 16 p.p.m. (see e.g. Fig. 8(d)). The broadness of the ^{29}Si MAS NMR signal is again characteristic for amorphous materials covering regions of different Si environments, but also for a distribution of bond angles and lengths [9].

It is well known that an increase in the average amount of Al bound to Si (m value in $Q^n(m\text{Al})$ describing a SiO_4 tetrahedron with n bridging oxygen atoms containing m Si–O–Al links) increases the chemical shift of the ^{29}Si NMR signal [9]. Literature values for amorphous Na-aluminosilicates are scarce, but -93.4 p.p.m. for $m = 2$ (Q^4(2Al)) and -88.7 p.p.m. for $m = 3$ (Q^4(3Al)) are reported [12]. In amorphous Mk m is about 1 [10, 13], so that the observed peak position of about -100 p.p.m. can be understood. By decreasing the Sil/Mk ratio k, the Al/Si ratio in the reaction mixture increases and a peak shift is thus expected if all Si and Al are consumed in IPG and assuming a uniform distribution of Al and Si on the molecular scale. In this work k is varied between 2.67 and 0.67, so that a variation of about 6 p.p.m. for the ^{29}Si chemical shift is expected according to literature values. However, for all studied mixing ratios, the measured chemical shift of IPG stays the same centred

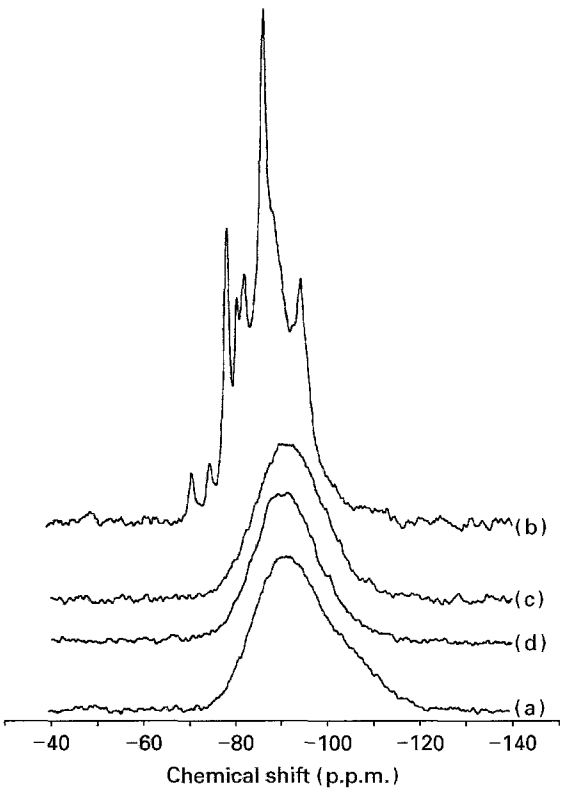

Figure 8 ^{29}Si MAS NMR spectra of LTIPG: (a) Sil/Mk = 0.7; (b) Sil/Mk = 2.7; (c) same as (b) but after washing; (d) Sil/Mk = 1.

at -91 p.p.m. leading to an approximate value for m between 2 and 3. This is illustrated in Fig. 8, where the ^{29}Si MAS NMR spectra of IPG prepared from reaction mixtures with different Si/Al ratios are shown. The down-field shift for all spectra compared to Mk (approximate peak position at -100 p.p.m.) is obvious. If the ratio Sil/Mk is below the stoichiometric value, an up-field tail is observed (Fig. 8(a)). This is due to unreacted Mk. Note that this effect is not seen in the ^{27}Al MAS NMR spectrum due to a too broad signal for the ^{27}Al nuclei in Mk. If the ratio Sil/Mk is beyond the stoichiometric value, residual silicate peaks are found (Fig. 8(b)). These disappear after rinsing the sample with water (Fig. 8(c)), and the remaining signal coincides with that for the stoichiometric Sil/Mk ratio ($k_{st} = 1$; Fig. 8(d)). So, the Al/Si ratio in IPG is related to a unique value and not to the Al/Si ratio of the initial reaction mixture. Only in stoichiometric reaction conditions with $k_{st} = 1$, all Al and Si from the reaction mixture is consumed completely in LTIPG.

At this moment, it can be concluded that the mean value of m in LTIPG remains constant for all initial Sil/Mk ratios of the reaction mixture. In combination with the ^{27}Al NMR observations, this value of m in LTIPG can be calculated by Equation 1

$$m = \frac{2n'}{2 + k_{st}s} \quad (1)$$

where n' is the cross-link density of Al in LTIPG ($n' = 4$), s is the ratio SiO_2/Na_2O in Sil ($s = 1.4$) and k_{st} is the stoichiometric ratio Sil/Mk ($k_{st} = 1$).

The value of m is then 2.35 according to Equation 1, meaning that the average Si environment is

Q^n(2.35Al). The cross-link density n of Si will be discussed in the next paragraph.

In Mk the cross-link density for the Si sites is four [10, 13, 14], while that for Al can not be defined because Al is present in different co-ordinations.

In IPG the cross-link density for Al was already proven to be four (see reasoning earlier in this section).

The reaction taking place in an alkaline aqueous medium, hydroxyl groups or other types of bound water could break Si–O–Si bridges thereby lowering the mean cross-link density for Si [15]. Indeed, such groups have to be found at Si sites, since tetrahedral Al preferentially occupies the sites with the lowest number of non-bridging oxygen atoms [15].

Preliminary cross polarization ^1H–^{29}Si CP NMR experiments reveal a weak signal indicating only a small amount of bound water (SiOH groups). This amount is estimated by TGA (see Section 2.2) to be about 2 wt% or 6% SiOH (on the total amount of Si–O bonds), lowering the cross-link density n from 4 to 3.76. So, the amount of bound water in LTIPG (z) is small compared to the total amount of water available in the reaction mixture ($z = 0.4 \ll w = 10$) and only a few non-bridging oxygen atoms are present in the inorganic polymer structure.

The observed ^{29}Si MAS NMR signal at -91 p.p.m. is consistent with the previous conclusion. For a Q^4(2.35Al) site, interpolation of the literature values [12] renders -91.8 p.p.m. Important differences in the cross-link density should shift this value by several p.p.m. A cross-link density of three instead of four for example would increase the chemical shift by about 10 p.p.m. Engelhardt and co-workers [12] even published a value of -74 p.p.m. for Q^3(2Al). The small deviation of the chemical shift of LTIPG (-91 p.p.m.) compared to the interpolated value of -91.8 p.p.m. is thus in agreement with the independent observation of the small amount of SiOH groups in this structure.

All foregoing arguments are a strong indication that the cross-link density for Si is close to four as is the case for Al. Therefore, IPG is a real aluminosilicate framework with a high cross-link density, justifying the nomenclature of (amorphous) inorganic polymer network.

All previous findings are in agreement with the model proposed by Engelhardt and Michel [9] for aluminosilicate glasses. In the case of LTIPG, however, a unique reaction stoichiometry exists, while other sodium aluminosilicate glasses can be composed out of almost any $Na_2O/SiO_2/Al_2O_3$ ratio [1, 16].

In conclusion, the combination of DSC results with ^{27}Al and ^{29}Si NMR leads to the following overall equation for the low-temperature production of a model LTIPG starting with a silicate solution and metakaolinite.

$$(Na_2O)(SiO_2)_{1.4}(H_2O)_x + (Al_2O_3)(SiO_2)_2(H_2O)_{0.05} \xrightarrow{\text{aq. } (<100\,^\circ C)} (Na_2O)(Al_2O_3)(SiO_2)_{3.4}(H_2O)_z$$

with z about 0.4.

3.3 Mechanical properties of the low-temperature inorganic polymer glass – mechanical testing.

The aim of this section is to investigate the influence of the mixing ratio Sil/Mk on the mechanical properties of LTIPG. The compositions used for mechanical testing differ from those analysed in the foregoing sections in the following aspects:

(i) the metakaolinite is an industrially produced one (A91), because of the limited availability of the standard kaolinite KGa-1.

(ii) a filler material is used to reduce the risk of crack formation due to the stresses introduced by water evaporation. The volume fraction of filler M32 (see Table I) is the same in all compositions (42%).

(iii) the concentration of the silicate solution is varied in such a way that for all compositions the water volume fraction in the fresh state is the same.

The strategy behind the last two conditions is to obtain compositions with almost the same porosity or capillary volume caused by the evaporation of water. It is known that porosity affects very much the strength values for ceramics (see e.g. the classical third power law of Powers for cement paste [17]). For a constant amount of water w in the silicate, the porosity would be the dominant factor in the mechanical properties of samples made from varying Sil/Mk ratios.

For purposes of comparison with mechanical properties, a new set of DSC measurements has been performed. The same clay and silicates as for the mechanical tests are used, but excluding the filler which does not affect the reaction nor its stoichiometry.

The mechanical results and reaction enthalpies are given in Table II and Fig. 9.

The compressive strength is strongly dependent on the sample composition as is clearly demonstrated in Fig. 9(a). The optimum mechanical properties are found for specimens prepared from the stoichiometric ratio (Sil/Mk = $k_{st} = 1$), both in dried and saturated conditions. The optimum in the compressive strength is not caused by differences in porosity since the apparent porosity of all samples is almost constant. It was shown in Section 3.2 that the molecular structure of LTIPG is not altered by changing the initial Sil/Mk ratio of the reaction mixture. So, the reason for the optimum lies in the fact that if a non-stoichiometric ratio is used, excess silicate or Mk is left after reaction. For Sil/Mk ratios smaller than one, Mk will remain after reaction. These Mk grains with a much lower compressive strength are incorporated and act as defects in IPG. For Sil/Mk ratios bigger than one, excess silicate will be homogeneously distributed in the network (mixed on a molecular scale) but will not contribute to the mean strength of the material. Note that the difference between bulk densities 1 and 2 (see Table II) seems to increase with an increasing Sil/Mk ratio, especially from a ratio of 1.2 onwards. These observations indirectly confirm the presence of residual silicate after non-stoichiometric curing, which is partially leached out during immersion.

TABLE II Results of mechanical testing[a] and reaction enthalpies for compositions according to Table I

Sil/MK	Compressive strength (MPa)		Bulk density ($g\,cm^{-3}$)		Apparent porosity[d]	Reaction enthalpy[e] ($J\,g^{-1}$)
	dried	saturated	1[b]	2[c]		
0.8	42.7 (4.5)	42.1 (2.5)	1.691 (0.006)	1.680 (0.004)	26.1 (0.1)	− 148
1.0	60.2 (2.4)	47.9 (2.1)	1.717 (0.012)	1.704 (0.012)	26.3 (0.0)	− 157
1.2	51.5 (0.5)	41.4 (2.1)	1.724 (0.004)	1.701 (0.002)	26.1 (0.1)	− 146
1.4	26.8 (1.1)	29.2 (1.3)	1.741 (0.014)	1.713 (0.010)	25.6 (0.1)	− 135
1.7	23.7 (0.5)	18.7 (0.6)	1.715 (0.021)	1.677 (0.014)	21.8 (0.3)	− 121

[a] All data are the mean of three measurements, with the standard deviation given between brackets.
[b] Bulk density 1 is the density measured on specimens dried at 105 °C immediately after curing.
[c] Bulk density 2 is the density measured after immersion in water for 24 h and subsequent heating to 105 °C.
[d] The apparent porosity is computed from the weights in saturated and dried states, supposing there is full saturation and open porosity.
[e] The absolute values for the reaction enthalpies are lower than those of Fig. 5(a) due to the differences in Mk and silicate concentration.

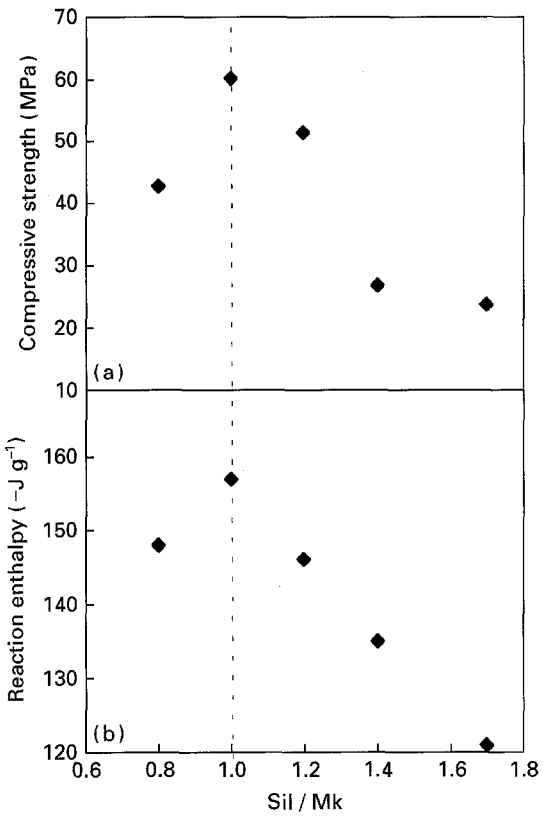

Figure 9 Compressive strength and reaction enthalpy of LTIPG as a function of the Sil/Mk ratio: (a) compressive strength; (b) reaction enthalpy.

Table II shows that the maximum reaction enthalpy is also reached for a Sil/Mk ratio of one as was expected (see Fig. 5). The DSC results obviously show the same trend as the mechanical properties (compare Fig. 9(a) and 9(b)) and illustrate the predictive force of "structure–property" relations.

4. Conclusions

It is demonstrated that at ambient temperature a "ceramic-like" material (LTIPG) can easily be obtained, starting from an aqueous silicate and a dehydroxylated clay. DSC and NMR indicate that the stoichiometry of the reaction is such that for each Al in metakaolinite one cation (Na^+) from the silicate has to be added.

Some important features of LTIPG's molecular structure are found by XRD and MAS NMR spectroscopy. It is proven that the material is an amorphous inorganic polymer network. The building blocks or "monomers" are SiO_4 and AlO_4 tetrahedra. No otherwise co-ordinated Al was detected. The monomers are combined in a more or less random way but with the restriction that each Al is surrounded by four SiO_4 groups so that no Al–O–Al bonds are present. The Si/Al ratio in LTIPG can not be influenced by a variable Sil/Mk ratio in the reaction mixture but corresponds to a unique stoichiometry. Less than 5% of the total amount of water of the Sil/Mk reaction mixture is incorporated in the inorganic network as SiOH bonds. This leads to the general formula of $(Na_2O)(Al_2O_3)(SiO_2)_{3.4}(H_2O)_{0.4}$ for the low-temperature synthesized aluminosilicate studied in this work.

This information is of importance to rationalize the mechanical properties of LTIPG materials produced from reaction mixtures with variable Sil/Mk compositions. A combination of characterization techniques enables the establishment of "structure–property" relations and the development of LTIPG materials with improved properties.

References

1. J. ZARZYCKI, "Glasses and the vitreous state" (Cambridge University Press, Cambridge, 1991).
2. J. E. MARK, H. R. ALLCOCK and R. WEST, "Inorganic polymers" (Prentice Hall, New Jersey, 1992).
3. G. A. PATFOORT, J. WASTIELS, P. BRUGGEMAN and L. STUYCK, in Proceedings Brittle Matrix Composites 2, September 1988, edited by A.M. Brandt and I.H. Marshall (Elsevier, London, 1989) p. 587.
4. G. A. PATFOORT and J. WASTIELS, "Greenhouse effect, sea level and drought" (Kluwer, 1990) p. 621.
5. H. RAHIER, B. VAN MELE and M. BIESEMANS, in Abstracts of the 12th European Experimental NMR Conference, Oulu, June 1994, edited by L.P. Ingman, J. Jokisaari, and J. Lounila, p. 125.
6. F. L. GALEENER, *J. Non-Cryst. Solids* **123** (1990) 182.
7. H. VAN OLPHEN and J. J. FRIPIAT "Data handbook for clay materials and other non-metallic minerals" (Pergamon Press, London, 1979).
8. H. RAHIER, B. VAN MELE and J. WASTIELS, *J. Mater. Sci.* **31**, 78–84.
9. G. ENGELHARDT and D. MICHEL, "High-resolution solid-state NMR of silicates and zeolites" (J. Wiley, Chichester, 1987).

10. J. ROCHA and J. KLINOWSKI, *Angew. Chem.* **102** (1990) 539.
11. J. ROCHA, J. KLINOWSKI and J. M. ADAMS, *J. Mater. Sci.* **26** (1991) 3009.
12. G. ENGELHARDT, M. NOFZ, K. FORKEL, F. C. WIHSMANN, M. MAGI, A. SAMOSON and E. LIPPMA, *Phys. Chem. Glasses* **26** (1985) 157; M. NOFZ, G. ENGELHARDT, F. C. WIHSMANN, K. FORKEL, M. MAGI and E. LIPPMA, *Z. Chem.* **26** (1986) 221.
13. R. H. MEINHOLD, K. J. D. MACKENZIE, and I. W. M. BROWN, *J. Mater. Sci. Lett.* **4** (1985) 163.
14. K. J. D. MACKENZIE, I. W. M. BROWN, R. H. MEINHOLD and L M. E. BOWDEN, *J. Amer. Ceram. Soc.* **68** (1985) 293.
15. T. UCHINO, T. SAKKA and M. IWASAKI, *J. Amer. Ceram. Soc.* **74** (1991) 306.
16. N. H. RAY, "Inorganic polymers" (Academic Press, London, 1978).
17. T. C. POWERS, *J. Amer. Ceram. Soc.* **41** (1958) 1.

Received 17 February
and accepted 15 August 1995